

Magnetic properties of nanocrystalline materials based on the system $(1 - x)\text{BiFeO}_3 - (x)\text{YFeO}_3$

© P.D. Kravtsova¹, M.V. Tomkovich¹, M.P. Volkov¹, I.V. Buryanenko², V.G. Semenov^{3,4}, V.I. Popkov¹, N.A. Lomanova¹

¹ Ioffe Institute,

St. Petersburg, Russia

² Peter the Great Saint-Petersburg Polytechnic University,

St. Petersburg, Russia

³ St. Petersburg State University,

St. Petersburg, Russia

⁴ Institute of Analytical Instrument Making, Russian Academy of Sciences,

St. Petersburg, Russia

E-mail: valdner347@gmail.com

Received May 19, 2023

Revised September 14, 2023

Accepted October 30, 2023

Nanocrystalline magnetically ordered materials based on bismuth and yttrium orthoferrites have been synthesized by the solution combustion method. The obtained materials demonstrate a significant difference between their magnetic properties and the properties of pure orthoferrites, in particular, a significant increase in the magnetic response.

Keywords: perovskites, bismuth orthoferrite, yttrium orthoferrite, nanocrystals, magnetization, Mössbauer spectroscopy.

DOI: 10.61011/PSS.2023.12.57682.5208k

1. Introduction

The materials development based on perovskite-like orthoferrites of bismuth and yttrium was of great interest for many years, since high-temperature multiferroics are relevant for various fields of technology, in particular, magnetoelectronics [1,2].

As it is known, bismuth orthoferrite (BiFeO_3) has a spatial modulation of magnetization, a spin cycloid with $\lambda_C = 62$ nm, the destruction of which is one of the important technological problems and occurs, in particular, with isomorphic substitution and reduction of particle sizes [1,3,4]. Yttrium orthoferrite (YFeO_3) has several structural modifications, which suggests variability in its functional characteristics [5]. Isomorphic replacement of BiFeO_3 structure in the bismuth sublattice with rare earth cations is one of the methods for suppressing the spin cycloid [1,4–8]. Functional properties of nanocrystals of variable composition $\text{Bi}_{1-x}\text{Y}_x\text{FeO}_3$ and $\text{Y}_{1-x}\text{Bi}_x\text{FeO}_3$ are considered in papers [6–12], which mainly present characteristics for narrow ranges x . The influence of the phase composition on the magnetic properties of materials of the system $(1 - x)\text{BiFeO}_3 - (x)\text{YFeO}_3$ is of interest from the point of view of the possibility to obtain new magnetic materials.

The purpose of this paper was to study the magnetic characteristics of nanocrystalline materials based on system of $(1 - x)\text{BiFeO}_3 - (x)\text{YFeO}_3$, obtained by glycine-nitrate combustion.

2. Samples synthesis and characterization

The samples $\text{Bi}_{1-x}\text{Y}_x\text{FeO}_3$ with rated value $x = 0.0 - 0.9$ were synthesized by glycine-nitrate combustion method [13–15]. The following sample markings are used: Y0 ($x = 0.0$), Y01 ($x = 0.1$), Y03 ($x = 0.3$), Y04 ($x = 0.4$), Y05 ($x = 0.5$), Y06 ($x = 0.6$), Y07 ($x = 0.7$), Y09 ($x = 0.9$).

The phase composition was determined on Rigaku Smart-Lab 3 diffractometer (CuK_{α} -radiation). The elemental composition was determined using FEI Quanta 200 scanning electron microscope with EDAX attachment. It was found that the average ratio of Bi/Y/Fe elements in samples Y0, Y01 and Y09 corresponds quite well to the rated one. In the Y03–Y07 samples with the highest content of iron-containing impurity phases of various structures (Figure 1), an excess of iron was recorded (δ), see Table 1.

X-ray diffraction patterns of the samples are shown in Figure 1. According to XRD data and EDX analysis, the main phase in samples Y0 and Y01 is isostructural to the rhombohedral phase BiFeO_3 (Table 1). Samples Y03–Y05 are composite particles based on the phases BiFeO_3 , YFeO_3 , Fe_2O_3 , Fe_3O_4 . Besides, most samples contain trace amounts of $\text{Bi}_2\text{Fe}_4\text{O}_9$, $\text{Bi}_{25}\text{FeO}_{39}$. The average crystallite size determined from the main reflexes of BiFeO_3 (012/110) and $o\text{-YFeO}_3$ (121/002) is given in Table 2. Due to the difficulty of separating the reflexes of the main phases BiFeO_3 and YFeO_3 in the sample Y05, Table 2 shows the average crystallite size for these phases.

Table 1. Elemental composition of samples of system BiFeO₃–YFeO₃

| Marking of sample | $x^*(Y)$ | Composition as per EDX-analysis | | | δ^{**} |
|-------------------|----------|---------------------------------|------|------|---------------|
| | | Bi | Y | Fe | |
| Y00 | 0 | 1.0 | 0.0 | 1.0 | 0.00 |
| Y01 | 0.1 | 0.91 | 0.09 | 1.02 | 0.02 |
| Y03 | 0.3 | 0.60 | 0.39 | 1.41 | 0.42 |
| Y04 | 0.4 | 0.43 | 0.57 | 1.53 | 0.53 |
| Y05 | 0.5 | 0.29 | 0.7 | 1.77 | 0.79 |
| Y06 | 0.6 | 0.21 | 0.59 | 1.51 | 0.89 |
| Y07 | 0.7 | 0.26 | 0.64 | 1.61 | 0.79 |
| Y09 | 0.9 | 0.07 | 0.85 | 1.33 | 0.45 |

Note. * rated value x , ** iron excess as per EDX data.

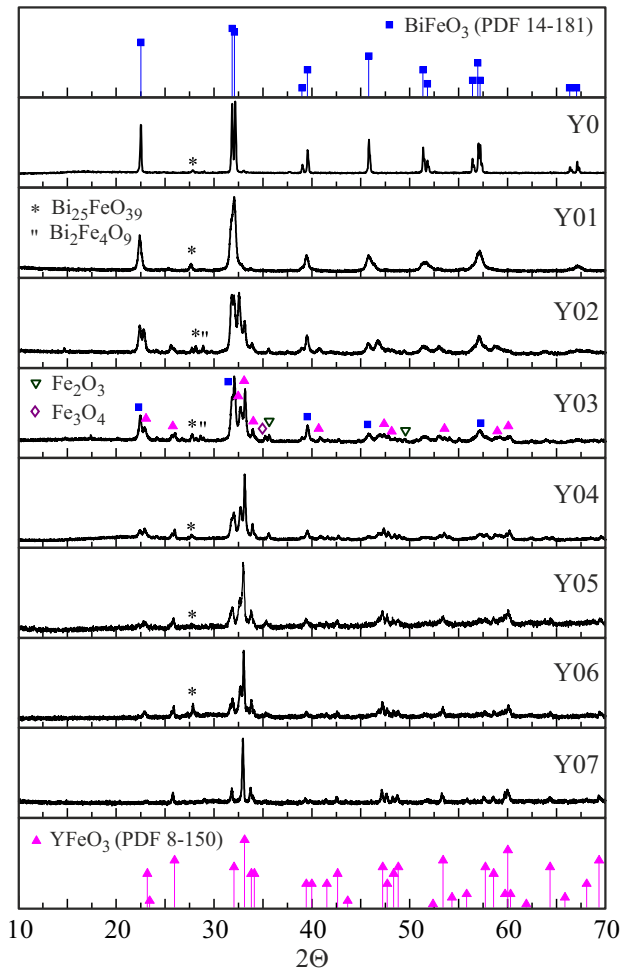
3. Methods of magnetic studies

The field dependences of magnetization M were measured at 300 K on a vibration magnetometer of PPMS system (Quantum Design). The Mössbauer study was carried out on WISSEL spectrometer at room temperature, in absorption geometry (source ⁵⁷Co in the rhodium matrix, the values of isomer shifts IS are given relative to IS α -Fe). For the magnetic experiment, doped materials Y01, Y05, Y09 were chosen, which have significant differences in composition, structure, morphology and content of iron-containing phases. The magnetic behavior of these samples was compared with samples of pure bismuth and yttrium orthoferrites.

4. Magnetic study results

4.1. Magnetometry

Figure 2 shows the magnetization curves $M(H)$ of samples Y01, Y05 and Y09, as well as of single-phase samples BiFeO₃ and YFeO₃. Hysteresis loops are observed for all materials, indicating the existence of magnetic order at room


Figure 1. X-ray diffraction patterns of samples of system BiFeO₃–YFeO₃.

temperature. Doped materials have a noticeably higher total magnetization M compared to pure orthoferrites. The curves $M(H)$ of doped samples are close to saturation already at 5 kOe, which qualitatively distinguishes them

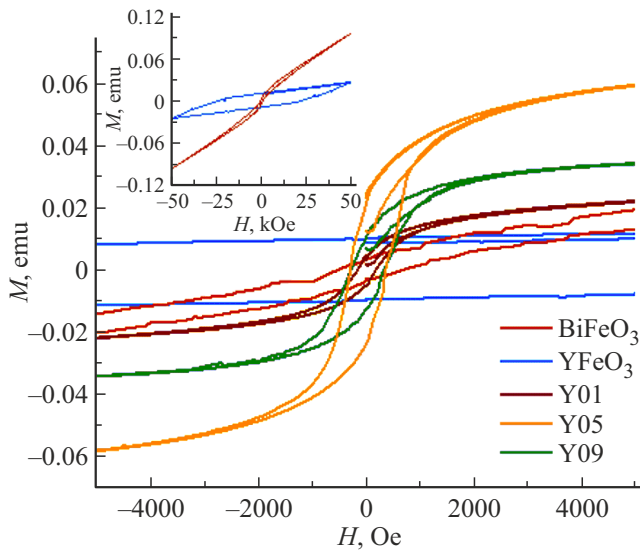
Table 2. Characteristics of samples of system BiFeO₃–YFeO₃ as compared with literature data

| Marking of sample | $x(Y_2O_3)$ | Volume of lattice cell V , Å ³ | | d , nm | M^* , emu/g (at 6 kOe, 300 K) | M_r , emu/g | H_c , kOe | Literature |
|-----------------------------|-------------|---|-------------------|----------|---------------------------------|---------------|-------------|------------|
| | | BiFeO ₃ | YFeO ₃ | | | | | |
| Y00 | 0 | 432 | — | 56 | 0.07 | 0.02 | 0.7 | This paper |
| BFO* | 0 | — | — | 55 | 0.09 | 0.03 | 1.738 | [7] |
| Y01 | 0.09 | 430 | — | 25 | 0.55 | 0.06 | 0.17 | This paper |
| BYFO10* | 0.1 | — | — | 50 | 0.1 | 0.02 | 0.957 | [7] |
| BYFO25* | 0.25 | — | — | 35 | 0.3 | 0.11 | 2.1 | [7] |
| Y05 | 0.29 | 428 | 230 | 64 | 8.3 | 1.9 | 0.36 | This paper |
| Y09 | 0.85 | — | 227 | 49 | 3.0 | 1.0 | 0.37 | This paper |
| <i>o</i> -YFeO ₃ | 1.0 | — | 224 | 41 | 0.01 | 1.0 | 23 | [13] |
| <i>o</i> -YFeO ₃ | 1.0 | — | 221 | 88 | 0.55 | 0.45 | 0.245 | [12] |

Note. M^* — magnetization value at applied magnetic field of 6 kOe and temperature of 300 K.

Table 3. Parameters of ^{57}Fe Mössbauer spectra of samples of system $\text{BiFeO}_3\text{--YFeO}_3$

| Sample | Component | $IS \pm 0.02$ (mm/s) | $QS \pm 0.03$ (mm/s) | $H_{\text{eff}} \pm 0.3$ (T) | A (%) | Phases |
|--------|-----------|----------------------|----------------------|------------------------------|---------|--------------------------------|
| Y05 | Doublet1 | 0.368 ± 0.032 | 1.808 ± 0.137 | – | 2.59 | BiFeO_3 |
| | Doublet2 | 0.328 ± 0.011 | 0.905 ± 0.026 | – | 5.71 | Nonmagnetic iron |
| | Sextet1 | 0.377 ± 0.004 | 0.176 ± 0.008 | 51.612 ± 0.026 | 13.33 | $\alpha\text{-Fe}_2\text{O}_3$ |
| | Sextet2 | 0.352 ± 0.002 | -0.000 ± 0.004 | 49.918 ± 0.018 | 49.96 | YFeO_3 |
| | Sextet3 | 0.325 ± 0.007 | 0.068 ± 0.009 | 48.622 ± 0.079 | 21.07 | Fe_3O_4 (A) |
| | Sextet4 | 0.709 ± 0.041 | -0.092 ± 0.042 | 46.285 ± 0.333 | 7.34 | Fe_3O_4 (B) |
| Y09 | Doublet1 | 0.317 ± 0.005 | 0.700 ± 0.016 | – | 1.94 | BiFeO_3 |
| | Doublet2 | 0.343 ± 0.004 | 1.178 ± 0.038 | – | 8.51 | Nonmagnetic iron |
| | Sextet1 | 0.31 ± 0.011 | 0.229 ± 0.022 | 51.603 ± 0.075 | 3.17 | $\alpha\text{-Fe}_2\text{O}_3$ |
| | Sextet2 | 0.357 ± 0.000 | 0.007 ± 0.001 | 49.985 ± 0.003 | 66.92 | YFeO_3 |
| | Sextet3 | 0.336 ± 0.002 | 0.022 ± 0.005 | 48.897 ± 0.049 | 14.44 | Fe_3O_4 (A) |
| | Sextet4 | 0.675 ± 0.006 | -0.002 ± 0.012 | 45.788 ± 0.044 | 5.03 | Fe_3O_4 (B) |

**Figure 2.** Magnetization curves of samples of the system $\text{BiFeO}_3\text{--YFeO}_3$ measured at 300 K.

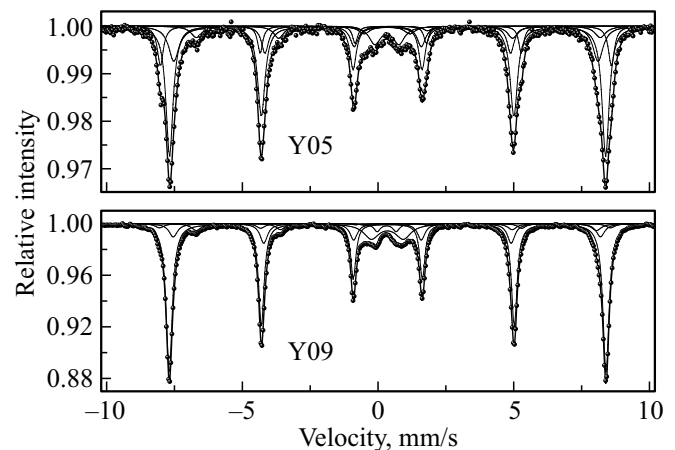
from the corresponding dependences of BiFeO_3 and YFeO_3 (see insert to Figure 2).

Based on the data from papers [3,4,6–11] and our earlier results on the influence of synthesis conditions on the magnetic properties of pure bismuth and yttrium orthoferrites [15,17], the increased magnetic response of materials $(1-x)\text{BiFeO}_3\text{--}(x)\text{YFeO}_3$ can be explained by the combined influence of the following factors. As it is known, BiFeO_3 nanoparticles with dimensions $d \leq \lambda_c$ have non-zero magnetization at room temperature. The increase in the magnetic response also occurs due to isovalent substitution in the bismuth sublattice. In our case, the size factor is responsible for the increase in magnetization, but is not the only one, since there is no obvious correlation of magnetic characteristics with the size of nanocrystals (see

Table 2). As can be seen from Figure 2, the magnetization of samples Y05 and Y09, containing excess iron according to EDX data (Table 1), is by several times higher than that of pure phases, and they have a narrower hysteresis loop. To clarify the factors that enhance the magnetism of these samples, data from Mössbauer study on the state of iron ions are given below.

4.2. Mössbauer spectroscopy

The Mössbauer spectra of the nanocomposite sample Y05 and the solid solution Y09, presented in Figure 3, are described by four sextets and two doublets (Table 3). The sextet parameters are characteristic of various iron-containing oxide phases, the main of which are $\alpha\text{-Fe}_2\text{O}_3$ [18], Fe_3O_4 [19] and YFeO_3 [13]. The main part of the substance in both samples contains iron atoms, which can be attributed to the magnetically ordered phase YFeO_3 , the content of which is higher in sample Y09.

**Figure 3.** ^{57}Fe Mössbauer spectra of samples Y05 and Y09.

The fraction of sextets attributed to iron oxides is higher in sample Y05, which is consistent with XPA and EDX data (Table 1). Apparently, the presence of a larger amount of the magnetite phase Fe_3O_4 ($\sim 30\%$) is responsible for the significant enhancement of the magnetic response of this material, and therefore it is probable type of magnetic order of yttrium-doped samples can be ferrimagnetism. Bulk iron oxide $\alpha\text{-Fe}_2\text{O}_3$ is antiferromagnetic, and its trace amount cannot make a significant contribution to the magnetism of the samples.

The parameters of doublet 1 in terms of values IS and QS are close to those known for nanocrystalline BiFeO_3 [15]. The small fraction of iron that characterizes doublet 2 may belong to some superparamagnetic X-ray amorphous phase accumulated in closed pores or at grain boundaries, and which may also contribute to magnetism.

Taken together with data on a significant increase in the magnetic response of yttrium-doped materials, the results obtained indicate the possibility of discovering new nanocomposite materials based on the system $(1-x)\text{BiFeO}_3-(x)\text{YFeO}_3$ near rated value $x \approx 0.5$. Nanocomposite particles of similar composition are practically not described in the literature and, due to their magnetic characteristics, may be of interest for practical use.

5. Conclusion

Using the glycine-nitrate combustion method, nanocrystalline materials based on the system $(1-x)\text{BiFeO}_3-(x)\text{YFeO}_3$ with crystallite sizes of 25–65 nm were synthesized. Mössbauer spectroscopy and magnetometry showed that the samples have magnetic order at room temperature and higher magnetization compared to pure bismuth and yttrium orthoferrites. The highest magnetization is demonstrated by a nanocomposite material with rated value $x \approx 0.5$, which has a wide hysteresis loop with $M_r \approx 1.9 \text{ emu/g}$. The enhancement of the magnetic response of the synthesized materials is associated with a combination of main factors — the destruction of the spin cycloid and the appearance of ferrimagnetism due to the formation of the magnetite phase in the samples.

Acknowledgments

The authors would like to thank corresp. member of RAS, Professor, Doctor of Chemical Sciences V.V. Gusarov (PTI RAS) for discussion of the results and scientific discussion.

Conflict of interest

The authors declare that they have no conflict of interest.

References

- [1] A.R. Akbashev, A.R. Kaul. *Uspekhi khimii* **80**, 12, 1211 (2011). (in Russian).
- [2] J. Wu, Zh. Fan, D. Xiao, J. Zhu. *J. Wang. Prog. Mater. Sci.* **84**, 335 (2016).
- [3] T.-J. Park, G.C. Papaefthymiou, A.J. Viescas, A.R. Moodenbaugh, S.S. Wong. *Nano Lett.* **7**, 766 (2007).
- [4] Z.A. Samojlenko, N.N. Ivakhnenko, E.I. Pushenko, V.Ya. Sycheva, N.A. Ledenev, A.V. Paschenko. *ZhTF* **91**, 5, 778 (2021). (in Russian).
- [5] I.I. Makoed, A.F. Revinsky, V.V. Lozenko, A.I. Galyas, O.F. Demidenko, A.M. Zhivulko, K.I. Yanushkevich, V.V. Moshchalkov. *FTT* **59**, 8, 1514 (2017). (in Russian).
- [6] A. Gautam, P. Uniyal, K.L. Yadav, V.S. Rangra. *J. Phys. Chem. Solids* **73**, 2, 188 (2012).
- [7] M. Hamed, Z. Mahmoud, F. Reza. *Appl. Phys. A* **124**, 11, 728 (2018).
- [8] N.A. Lomanova, M.V. Tomkovich, A.V. Osipov, V.V. Panchuk, V.G. Semenov, I.V. Pleshakov, M.P. Volkov, V.V. Gusarov. *FTT* **61**, 12, 2503 (2019). (in Russian).
- [9] S. Lokesh, B. Falguni, K. Priyanka, M. Roy. *J. Electroceram.* **44**, 195 (2020).
- [10] O. Rosales-González, F. Sánchez-De Jesús, F. Pedro-García, C.A. Cortés-Escobedo, M. Ramírez-Cardona, A.M. Bolarín-Miró. *Materials* **12**, 13, 2054 (2019).
- [11] W. Zhang, C. Fang, W. Yin, Y. Zeng. *Mater. Chem. Phys.* **137**, 3, 877 (2013).
- [12] A.N. Sokolova, O.V. Proskurina, D.P. Danilovich, V.V. Gusarov. *Nanosyst. Phys. Chem. Math.* **13**, 1, 87 (2022).
- [13] V.I. Popkov, O.V. Almjasheva, V.N. Nevedomskiy, V.V. Panchuk, V.G. Semenov, V.V. Gusarov. *Ceram. Int.* **44**, 17, 20906 (2018).
- [14] A.A. Ostroushko, T.Yu. Maksimchuk, A.E. Permyakova, O.V. Russkikh. *Zhurn. neorgan. khimii* **67**, 6, 727 (2022). (in Russian).
- [15] N.A. Lomanova, V.V. Panchuk, V.G. Semenov, I.V. Pleshakov, M.P. Volkov, V.V. Gusarov. *Ferroelectrics* **569**, 1, 240 (2020).
- [16] I.Ya. Mittova, N.S. Perov, Yu.A. Alekhina, V.O. Mittova, A.T. Nguyen, E.I. Kopeichenko, B.V. Sladkoptev. *Neorgan. materialy* **58**, 3, 283 (2022). (in Russian).
- [17] V.I. Popkov, O.V. Almjasheva, A.S. Semenova, D.G. Kellerman, V.N. Nevedomskiy, V.V. Gusarov. *J. Mater. Sci.-Mater. Electron.* **28**, 10, 7163 (2017).
- [18] I.S. Lyubutin, C.R. Lin, Yu.V. Korzhetskiy, T.V. Dmitrieva, R.K. Chiang. *J. Appl. Phys.* **106**, 3, 034311 (2009).
- [19] H.Y. Hah, S. Gray, C.E. Johnson, J.A. Johnson, V. Kolesnichenko, P. Kucheryavy, G. Goloverda. *J. Magn. Magn. Mater.* **539**, 168382 (2021).

Translated by I.Mazurov